CHARACTERIZATION OF DETONATION WAVE PROPAGATION IN LX-17 NEAR THE CRITICAL DIAMETER

T. D. Tran, C. M. Tarver, J. Maienschein, P. Lewis, M. Moss, R. S. Lee, and F. Roeske
Lawrence Livermore National Laboratory
Livermore, CA 94551

A new Detonation Profile Test (DPT) was developed to measure simultaneously the detonation wave breakout profile and the average detonation velocity at the breakout surface. The test evaluated small cylindrical samples with diameter up to 19.08 mm and length up to 33 mm. The experiment involved initiating a LX-17 cylindrical specimen and recording the wave breakout using a fast streaking electronic camera. The initiation was done using a PBX-9407 pellet (1.630 g/cm^3), which has a Chapman-Jouguet (C-J) pressure close to that of LX-17. The acceptor breakout surface had a 2 mm wide by 1 mm deep groove that provided a step in the recorded breakout profile for velocity determination. Results for 12.7 mm diameter unconfined LX-17 charges showed detonation velocity in the range between 6.79 and 7.22 km/s for parts up to 33 mm long. Since LX-17 cannot sustain detonation at less than 7.3 km/s, these waves were definitely failing. Experiments with confined 12.7 mm diameter and unconfined 19.08 mm diameter samples showed wave velocities in the range of 7.3-7.6 km/s, values approaching steady state conditions at infinite diameter. Both unconfined and confined charges show no sensitivity to density variations in the range between 1.890-1.915 g/cm^3. Experiments with 15.88 mm and 19.08 mm diameters gave velocities in the range between 7.2-7.45 km/s, values close to that expected for failure. The velocity measurement has an estimated experimental error in the range of 2%, which is large enough to complicate data analysis. Calculations using the Ignition and Growth model for LX-17 were compared to the results. The effects of density, confinement and charge diameter on wave breakout profiles and detonation wave velocity were accurately reproduced. A comparative analysis of the experimental breakout patterns and the calculated wave curvatures for the densities and dimensions was also determined.

INTRODUCTION

The detonating shock wave in insensitive high explosive charges such as LX-17 (92.5 wt% TATB, 7.5 wt% Kel-F 800) requires a finite initiation cross section (diameter) and run distance to propagate and build up to steady state conditions. This minimum area is defined by the failure diameter below which detonation waves cannot be sustained. The failure diameter for LX-17 has not been measured experimentally; and factors which affect the detonation behavior in the region near the failure conditions are not well understood.

The relationship between the failure diameter and the detonation wave velocity for two TATB-based formulations was reported by Campbell and Engelke.[1,2] The failure diameters at room temperature for two Kel-F 800 bonded composites containing 90 wt% and 95 wt% dry aminated TATB were determined to be 15 and 9 ± 1 mm, respectively. A linear interpolation suggests that the failure diameter for LX-17 is approximately 12 mm. The build up to detonation in these unconfined charges is a transient process and is dependent on the length of the charge and the extent to which the charge diameter exceeds the failure diameter. The required run distance needed

to develop full detonation is dependent on how much energy is being lost at the boundary. In cases where the charge diameter is close to failure, several hundred mm might be needed before the shock wave either reaches steady state or dies out. [1,2] The behavior of the detonation process in this transient region is not well understood. It is speculated that the dependence of the detonation wave parameters such as velocity and wave curvature near failure is highly dependent on the material heterogeneity such as density and particle size. If such transient phenomenon can be characterized accurately and reproducibly, it will provide useful insights on how changes in material properties would affect detonation performance in these charges.

The study of the detonation phenomena in small insensitive high explosive charges near the failure diameter is of academic and practical interest. The initiability of LX-17 and its buildup to detonation under such conditions are not completely understood. Most experiments have involved large charges (cylinder test, divergence test) whose diameters are significant larger than failure conditions. Models have described these full detonation conditions well. On the other hand, the understanding of the transient process prior to steady state detonation, especially those close to failure in small charges, is limited. Additional data in this regime would enable modelers to expand and/or fine tune existing models describing the processes associated with the buildup to full detonation.

There is also a need to develop a test to characterize the performance of IHE charges in as small a sample as possible. Such an experiment can allow workers to investigate a larger parameter space with many more experiments and can leverage availability of many existing samples,[3] especially simulated aging specimens in which one or more properties can be tailored.

PBX 9407 was selected as the booster material because it has a Chapman - Jouguet pressure of 275 Kbar (at 1.63 g/cm^3), comparable to that for LX-17. Such a manner of boosting should facilitate a rapid transition to steady state and minimize gap effects. The divergence test performed at Pantex has a similar initiation chain where a 12.7 mm diameter x 12.7 mm long pellet has been used to successfully boost LX-17 charges[4]. The smaller Detonation Profile Test (this work), which requires an order of magnitude smaller specimen than that required in Pantex Divergence test, will leverage a wealth of characterization information in a propagation regime that has received little study. The test is also easily extended to study other IHE materials such as PBX-9502 and UF-TATB, because both of these materials have failure diameter smaller than that of LX-17.

EXPERIMENTAL

A schematic of the Detonation Profile test set-up, a picture of a pressed LX-17 specimen and a resulting streak record are shown in Figure 1. The test involves initiating a cylindrical (e.g. 12.7 mm diameter x 25.4 mm long, 6.1 g) LX-17 test specimen with a PBX-9407 booster (12.7 mm diameter x 12.7 mm long). The booster is initiated by a RP-2 Exploding Bridgewire Detonator (RISI, Reynolds Industries, Inc.). A rectangular groove 2 mm wide x 1 mm deep was machined into one of the sample surface. This surface is illuminated with 532 nm laser light. A streak camera, looking perpendicular to the notched surface, records the extinction of the laser light as the wave breaks out on the surface. This technique provides us with a high-resolution spatial and temporal profile of the emerging detonation wave as well as the timing between the bottom and top surfaces of the groove. The breakout of the detonation front at the surface of the LX-17 sample is observed through a thin slit (represented by a line ABCD in the figure) perpendicular to the groove. The resulting streak camera record (see Figure 1) shows the wave arrival at the bottom of the groove (between B and C), its propagation along the groove wall and finally breaking out on both sides of the groove opening (from B and C to A and D). The difference in the arrival time between the bottom and at the surface (extrapolated to middle of the groove) along with the measured travel distance (groove depth) is used to calculate the average detonation velocity in this final 1 mm region.

The groove depth was measured using a contact Bausch and Lomb DR-25C Optical Gage. A series of precision gage blocks are used to calibrate the system. A series of 4 measurements were made on the surface of the specimen and at the center in the groove in order to calculate the groove's depth. Recent groove depth measurements used a non-contact high-definition optical profilometer (Conoprobe 1000, Optimet Optical Metrology Inc, MA). The groove depth was calculated from a scan perpendicular to the groove through the center. Both techniques gave comparable results (± 3 microns).
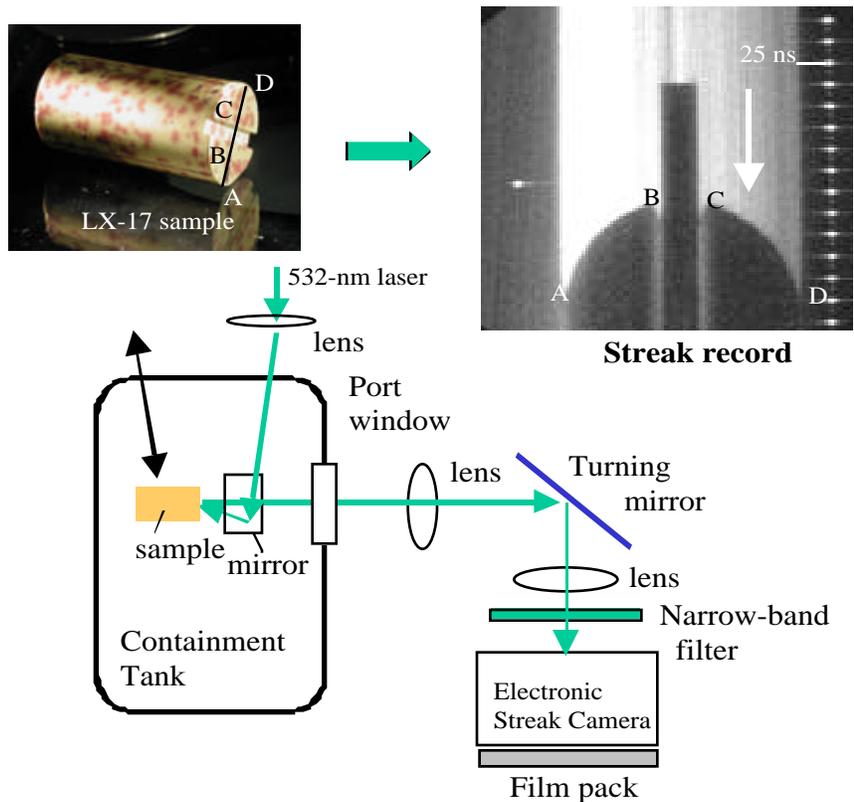
FIGURE 1. A PICTURE OF THE SLOTTED LX-17 SAMPLE, THE RESULTING STREAK CAMERA RECORD AND A SCHEMATIC OF THE EXPERIMENTAL SET-UP.

The optical profilometer, however, is more accurate and is used as the standard technique. In samples subjected to thermal cycling to produce the Ratchet growth-induced density changes (described below), the groove depth was measured after thermal cycling.

LX-17 cylindrical specimens were machined from larger cores that were obtained from hydrostatically pressed billets. The billets were made from two main lots of LX-17-1 so as to minimize lot-to-lot variations. As the result, all specimens have similar processing history and are expected to be fairly homogeneous in terms of density uniformity. Special machining procedure was used to keep the top and bottom surfaces of the cylindrical samples flat and parallel to within 12.5 microns. A 2-mm diameter end mill was used to cut a 2 mm wide x 1 mm deep groove across the center of one surface. Inspection of the surface and the groove profile by the optical profilometer shows that the surface was within specifications and that the groove had a flat bottom and perpendicular wall.

Thermal cycling is used to produce specimens at lower densities from higher density machined samples. Thermal treatment has been observed to induce irreversible expansion in IHE composites (Ratchet growth)[5] and effectively reduce the bulk density. This approach was used here to reproducibly and conveniently prepare specimens with precise densities. Samples were typically thermally cycled between - 50℃ and 70℃ at a rate of 1℃ per minute until the desired density was reached. The parts were first cycled to cold temperature limit from initial ambient temperature. The dwell time at - 50℃, 23℃ and 70℃ was one hour at each limit. Bulk sample densities could be reduced by as much as 2% over 40 cycles.

Specimen density was measured by an immersion density technique. This density measurement method is widely used and the accuracy and reproducibility are excellent but are highly dependent on calibration, correction and operator care. A short summary of the procedure is described below. Details are available elsewhere.[5] The

experimental setup included a Mettler AE 163 electronic balance, accurate to 0.1 mg, which allowed for both dry (in air) and wet (in a water bath) weighing of specimens. A stainless steel wire mesh basket, suspended from the underside of the balance and fully submerged in a 6-liter water bath, allowed the totally immersed sample to be weighed. Concentric strips of wire screen, placed inside the water batch to act as a baffle for water movement, minimize turbulence during weighing. The fluid in the bath was distilled water, to which 0.1% by volume of the wetting agent Aerosol OT had been added to aid in the elimination of bubbles adhering to the submerged sample. The actual density of the water in the bath was calculated by means of a glass standard of known density (an 1826b soda lime standard reference material). The immersion densities of the specimens were corrected for water temperature, air pressure and humidity and were reported at standard temperature and pressure conditions (21°C and 760 mm Hg).

RESULTS AND DISCUSSION

Initial experiments were conducted with unconfined LX-17 charges at 12.7 mm diameter. The effects of length, density, confinement and diameters were investigated to explore the variance in shock wave velocity and wave curvature.

EFFECTS OF PBX-9407 BOOSTER SIZE

Initiability of unconfined 12.7 mm diameter x 25.4 mm long LX-17 cylinders was observed to be highly dependent on the booster length. Several tests with 12.7 mm diameter x 6 mm thick booster pellets failed to initiate the LX-17 pellets. Tests with a stack of two 6 mm booster pellets (12 mm total length) all successfully initiated the LX-17. To minimize gap effects and simplify the test set-up, a single booster pellet 12.7 mm long was selected for subsequent experiments. The breakout profiles of several 12.7 mm diameter PBX 9407 booster pellets with different length are shown in Figure 2. The difference in the curvature of a single 6 mm pellet and that from two 6 mm pellets (12 mm long) is significant, amounting to over 100 ns lag at the edge. The single booster pellet at 12.7 mm long showed the flattest wave front. The failure to initiate LX-17 by a 6 mm PBX 9407 pellet suggests that the observed wave front was not sufficient to deliver adequate momentum across the whole contact surface.
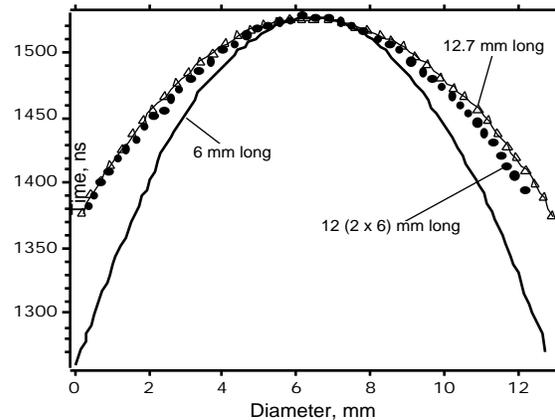

FIGURE 2. BREAKOUT PROFILES OF PBX 9407 BOOSTERS AT 12.7 mm DIAMETER AND DIFFERENT LENGTH.

EFFECTS OF SAMPLE LENGTH

The detonation wave velocities and the propagation of the shock wave in unconfined 12.7 mm charges were investigated over several lengths between 12.7 and 33 mm. In these experiments, the PBX 9407 booster was composed of two 12.7 mm diameter x 6 mm-thick pellets. The detonation velocities (Figure 3) decrease slightly from 7.22 km/s at 12.7 mm to 7.02 km/s at 33 mm. The velocities are significantly lower than 7.3 km/s, suggesting that they are decaying. One experiment was repeated using a single 12.7 mm booster pellet, yielding a larger velocity (7.42 km/s). The experimental error in the velocity determination is estimated to be about 2%. This comes from uncertainties in the determination of the arrival times from the digitized streak camera record. This relatively high standard error complicates the analysis of the data. However, the results are in line with our expectation that LX-17 failure diameter is approximately 12.7 mm. The initiation conditions in this region are highly sensitive to initiation input pressure, the pressure profile and the sample length. The breakout profiles of the emerging shock waves are included in Figure 4 together with the input PBX 9407 wave front. The wave centers are superimposed for comparison purpose. While the wave front appears to evolve to flatter profile with increasing sample length, the comparison is complicated by some asymmetry in the breakout profiles. The recorded wave fronts do not suggest slowly decaying waves, for which, the lags at the edges (relative to the center of the profile) should increase in longer samples. It is
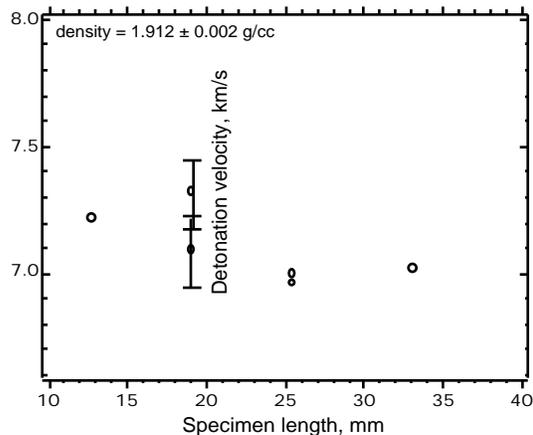
FIGURE 3. VELOCITY AS FUNCTION OF SPECIMEN LENGTH IN UNCONFINED 12.7 mm DIAMETER LX-17. PBX 9407 BOOSTER IS 12 mm LONG (2 X 6 mm PELLETS). ALL VALUES HAVE SAME ERROR.

FIGURE 4. EFFECT OF LENGTH AT 12.7 mm DIAMETER ON DETONATION WAVE VELOCITY AND CURVATURE. BOOSTER IS 12 mm LONG (2 X 6 mm PELLETS).

possible that the wave profile would become flatter as the velocity at the center decays slowly.

DENSITY EFFECTS

Several tests at distinct density ranges were completed to explore the test sensitivity to density variation. The measured detonation velocities in unconfined 12.7 mm diameter x 25.4 mm long samples are shown in Figure 5. The velocities vary between 7.18 and 7.45 km/s for the density range between 1.895 and 1.915 g/cm^3 and do not show the expected increase with higher density. The expected dependence of the steady state detonation velocity on LX-17 density in the density range studied here is small (~ 0.08 km/s).[2,6] This is complicated by a rather large experimental error inherent in the velocity measurement (~ 2%). It may well be that the large variances in the measured velocities are characteristics of the transient processes near the failure diameter.

Experiments with unconfined larger charges (19.08 mm diameter by 33 mm long) were also completed to obtain test reproducibility and minimize possible difficulties in measuring velocity near the critical diameter as observed above. The results are included in Figure 5. The reproducibility is about the same magnitude as the experimental error observed at 12.7 mm diameter. This variance apparently reflects the experimental error in the velocity measurement. Since the velocity variation
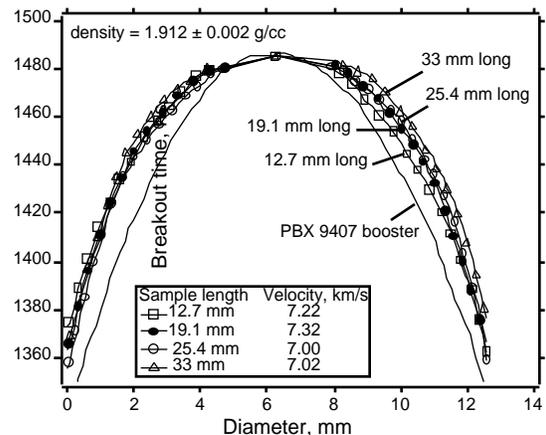
over the density range of interest here is in the range of 1%, the accuracy of the measurement has to be improved significantly to enhance the test sensitivity.

A comparison of the detonation profiles for a failing detonation wave (velocity at 7.00 km/s) and one closer to steady detonation (velocity at 7.45 km/s) is shown in Figure 6. The difference in the curvature is significant. The difference in the arrival times of the edge of the sample is about 15 nanoseconds. This is compared to about 120 nanoseconds total lag time between the center and the edge of the specimen. Such a difference in the profiles is consistent with that predicted by the Ignition and Growth model as shown in a later section. The results demonstrate a reasonable level of sensitivity in the wave front variances with density that can be measured in this test. The wave breakout profiles are reproducible with an error of about 2 ns.

EFFECTS OF CONFINEMENT

The effect of confinement on 12.7 mm diameter charges is included in Figure 5. The confinement was established using 6.4 mm thick concentric Teflon tube to enclose the LX-17 charges. The measured velocities for confined samples (25.4 mm long) did not show a clear increase in shock velocity compared to those in unconfined samples. There is an increase in the velocities in the two densest samples. Additional data are obviously needed to clearly elucidate the effect of confinement. The wavefront
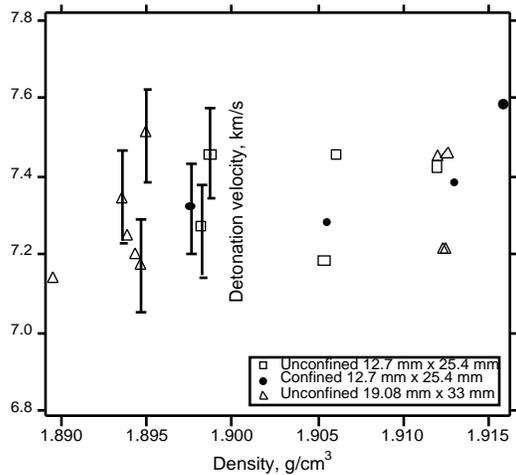
FIGURE 5. EFFECTS OF DENSITY ON VELOCITY FOR UNCONFINED AND CONFINED 12.7 mm DIA. CONFINEMENT USED 6.4 mm THICK TEFLON SLEEVE (SEE TEXT). ERROR BAR REPRESENTS 2% (ONE STANDARD DEVIATION). ALL VALUES HAVE SAME ERROR.

curvatures are flatter in confined samples as expected. (e.g., Figure 8).

DIAMETER EFFECTS

The diameter effect curve for these samples is shown in Figure 7. A line drawn between the velocities for the infinite diameter and the estimated failure diameter of LX-17 is used as an expected dependence of the steady state velocity in these samples. Cylinder experiments at 1/R of 0.03937 (50.8 mm diameter) gave velocity of 7.63 km/s.[6] From the work of Campbell and Engelke[1,2], the infinite diameter detonation velocity of LX-17 is estimated to be 7.68 km/s and the minimum detonation velocity near failure is estimated to be approximately 7.3 km/s. The detonation velocities for unconfined LX-17 samples in this work all fall below the expected linear relationship established above. Without additional data taken at longer run distances, it is not possible to conclude here that the data for experiments at 15.88 mm and 19.08 mm diameter charges represent a failing shock wave phenomenon. Plans are under way to overdrive the LX-17 charges and to add more diagnostics to study the behavior of these transient detonation waves to gain additional insights into the complex mechanism of detonation failure.
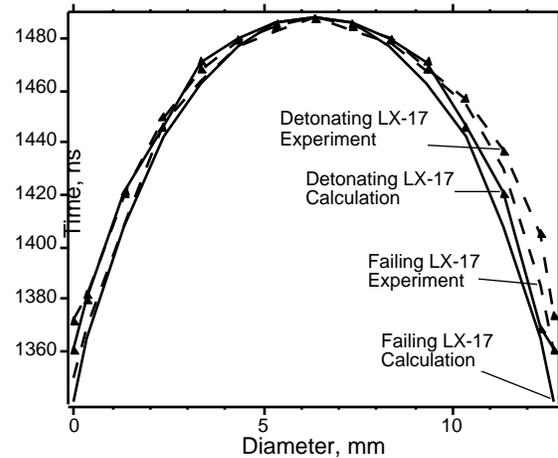

FIGURE 6. COMPARISON OF THE EXPERIMENTAL (DASHED LINES) AND CALCULATED DETONATION WAVE BREAKOUTS (SOLID LINES) FOR A FAILING WAVE AND ONE NEAR FAILURE IN UNCONFINED 12.7 mm DIAMETER X 25.4 mm LONG LX-17 SAMPLES.

IGNITION & GROWTH MODELING

The Ignition and Growth reactive flow model of shock initiation and detonation of solid explosives has been incorporated into several hydrodynamic computer codes and used to solve many 1D, 2D, and 3D explosive and propellant safety and performance problems.[7-12] The model uses two Jones-Wilkins-Lee (JWL) equations of state, one for the unreacted explosive and one for its reaction products, in the temperature dependent form:

$$p = A e^{-R_1 V} + B e^{-R_2 V} + \omega C_V T/V \qquad (1)$$

where p is pressure in Megabars, V is relative volume, T is temperature, ω is Gruneisen coefficient, C_V is the average heat capacity, and A, B, R_1, and R_2 are constants. The reaction rate law for the conversion of explosive to products is:

$$dF/dt = I(1-F)^b (\rho/\rho_o - 1 - a)^x + G_1(1-F)^c F^d p^y$$
$$(0 < F < F_{igmax}) \qquad (0 < F < F_{G1max})$$

$$+ G_2(1-F)^e F^g p^z \qquad (2)$$
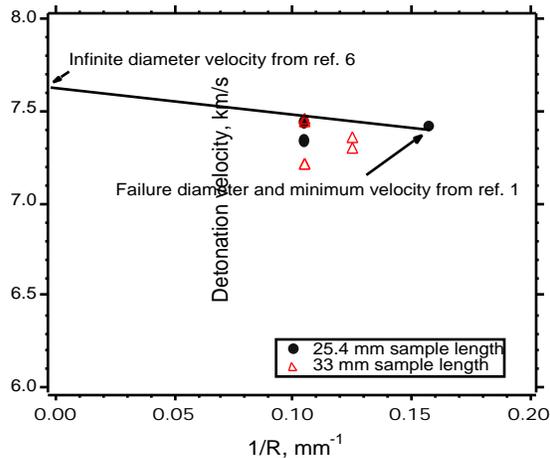$$(F_{G2min} < F < 1)$$

FIGURE 7. MEASURED DETONATION WAVE VELOCITIES AT THREE DIAMETERS AND 2 DIFFERENT SAMPLE LENGTHS.

where F is the fraction reacted, t is time, is the current density, $_o$ is the initial density, and I, G_1, G_2, a, b, c, d, e, g, x, y, z, F_{igmax}, F_{G1max} and F_{G2min} are constants. The mixture equations for the Ignition and Growth assume pressure and temperature equilibration between the unreacted explosive and the reaction products.

This three term rate law models the three stages of reaction generally observed in shock initiation and detonation of heterogeneous solid explosives. For detonation, the first term represents the ignition of the explosive as it is compressed by the leading shock wave creating heated areas (hot spots) as the voids in the material collapse. The fraction of explosive ignited is approximately equal to the original void volume. The second reaction models the rapid formation of the major reaction product gases (CO_2, N_2, H_2O, CO, etc.). The third term is used to describe the relatively slow diffusion controlled formation of the solid carbon particles in the form of diamond, graphite, or amorphous carbon. For TATB-based explosives, the last 20% of the energy release is assumed to be solid carbon formation. The LX-17 Ignition and Growth parameters and the ideal Chapman-Jouguet (C-J) detonation JWL parameters for the PBX 9407 booster explosive used in this study are given in companion papers.[13,14] The mesh sizes used in these calculations are 10 and 20 zones per mm. The calculations are independent of mesh size so they have converged.

Ambient temperature data are compared to Ignition & Growth predictions in the next Section.

COMPARISON OF EXPERIMENTAL AND IGNITION & GROWTH RESULTS

This Section shows the comparisons between Ignition & Growth calculations and the experimental data described previously. The 6 mm, 12 mm, and 12.7 mm long PBX 9407 booster charges were modeled as ideal C-J detonations, because their measured wave curvatures shown in Fig. 2 and detonation velocities agreed closely with C-J calculations. These curved wave fronts were then used to initiate LX-17 charges of various lengths, diameters, initial densities, and initial temperatures tested experimentally. Based on cylindrical rate stick data on PBX 9502,[2] the failure diameter of ambient temperature LX-17 was calculated to be >11 and <12 mm when initiated by a planar detonation wave.[8] When initiated by the curved PBX 9407 waves used in this study, the failure diameter of LX-17 should be slightly larger. As discussed in the Experimental Section, 12.7 mm diameter charges of LX-17 proved to be very close to failure. Since the lowest detonation velocity measured by Campbell[2] was 7.387 mm/µs and the estimated infinite diameter detonation velocity of LX-17 is less than that of PBX 9502 (7.680 versus slightly >7.716, the 108 mm diameter value for PBX 9502), any measured detonation velocities less than 7.3 mm/µs at the end of the LX-17 cylinders should be indicative of failing waves. Ignition & Growth calculations show that the maximum length of LX-17 used in this study (33 mm) is not long enough to observe complete failure or buildup to steady state detonation using either a p^2 or p^3 dependence in the second rate in Eq. (2).

The calculated wave curvatures for a failing wave and a propagating detonation in 12.7 mm diameter, 25.4 mm long LX-17 cylinders are compared to the corresponding experimental records in Fig. 6. The calculations are by definition axially symmetric while the experimental records exhibit some asymmetry. Overall the calculated curvatures agree closely with the experimental measurements. The calculations showed slightly longer time delays at the cylinder edge than did the experiments. This may be due to the experimental difficulties in observing light from the very edges of the cylinders or too slow a carbon formation reaction rate in the third term of Eq. (2) causing the calculated curvatures at the edges to be slightly long.

The effects of 6.35 mm of Teflon confinement on the experimental and calculated curvatures of 12.7 mm diameter, 25.4 mm long LX-17 cylinders are shown in Fig. 8. The Teflon confinement definitely decreases the wave curvature in both the experiments and the calculations. The experimental record for Teflon confinement is also slightly asymmetric, but the agreement between calculation and experiment is still excellent. As in Fig. 8, the calculated arrival times at the edges of the cylindrical charges are longer than experimental times by about 10 ns compared to approximately 130 ns total arrival time differences between the center and edge of the LX-17 cylinders. The LX-17 detonation model correctly predicts the expected changes in wave curvature for Teflon confinement, as it did for PMMA and copper confinement in cylinder tests[13] and for spherically diverging detonation waves.[13,14]

At a diameter of 19.08 mm, ambient temperature LX-17 definitely detonates. Fig. 9 shows the experimental and calculated curvatures for 25.4 mm long, 19.08 diameter LX-17 charges. The experimental record is shown in Fig. 9 as with the calculated wave curvature for unconfined LX-17 at this diameter. In the 19.08 mm diameter case, the Ignition & Growth model predicted slightly less curvature than the experiments, but the overall agreement is excellent. Additional experiments are needed to get meaningful statistics on wave curvature
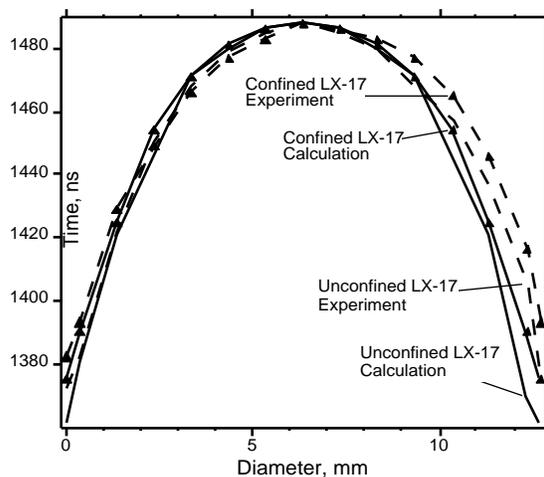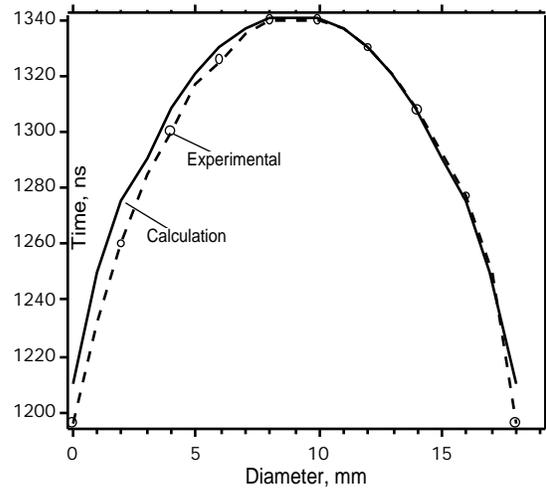

FIGURE 9. EXPERIMENTAL AND CALCULATED LX-17 DETONATION WAVE CURVATURES FOR UNCONFINED 19.08 mm DIAMETER CYLINDERS.

variations, and additional calculations are needed to further test the LX-17 reaction rates and equations of state.

Some of the LX-17 cylinders pressed to higher densities (1.912-1.915 g/cm^3) exhibited low detonation velocities and appear to be failing. A significant increase in failure diameter as the theoretical maximum density (TMD) is approached is a well-known experimental observation, especially for carbon rich molecules like TATB and TNT.[16] An LX-17 Ignition & Growth calculation predicted failure of a 12.7 mm diameter cylinder with an initial density of 1.914 g/cm^3 and 1.5 % reacted in the ignition term of Eq. (2), as hot-spot theory would estimate for a TMD of 1.944 g/cm^3. The LX-17 Ignition & Growth model predicts a failure diameter of >13 and <14 mm for 1.914 g/cm^3 with 1.5% ignited. Thus Ignition & Growth model appears to correctly predict the failure diameter versus initial density curve by changing only the fraction ignited by the ignition term in direct proportion to the initial void volume, but more experiments at higher densities and larger diameters are required to be certain.

CONCLUSIONS

The detonation velocity and wave curvature of LX-17 materials with diameters up to 19.08 mm and

FIGURE 8. EXPERIMENTAL AND CALCULATED LX-17 DETONATION WAVE CURVATURES FOR 12.7 mm DIAMETER, 25.4 mm LONG UNCONFINED AND TEFLON CONFINED CHARGES.

lengths up to 33 mm were measured using a new Detonation Profile experiment. The results showed that the leading detonation wave behavior is dependent on the booster length, the confinement, the sample diameter and length, and the density. Detonation in unconfined 12.7 mm diameter yields velocities well below the expected steady state value and little detectable sensitivity to density. The results are attributable to behavior near LX-17 failure diameter. Confinement with 6.4 mm thick Teflon sleeves produced slightly larger velocities and broader wave breakouts. Tests with unconfined 15.88 mm and 19.08 mm diameters did not show conclusively the expected higher velocities compared to the unconfined 12.7 mm diameter. The error in the velocity measurement was estimated at 2%, which is larger than the variability observed. The low detonation velocities in most samples in this range suggest that the developing shock wave is not yet exhibiting steady state behavior. These waves are either slowly failing or slowly building up to steady state. Overdriving the LX-17 cylinders with higher-pressure HMX-based plastic bonded explosives will determine which phenomenon is happening. Experimental error in the velocity measurements over a small run distance and in small samples is very significant. While the experiment demonstrates simultaneous measurements of key detonation parameters in small samples, the value of the test is limited thus far by the ability to measure the detonation velocity accurately.

ACKNOWLEDGEMENT

REFERENCES

1. Campbell, A. W. and R. P. Engelke, *Sixth International Detonation Symposium on Detonation*, ACR-221, p. 642, Office of Naval Research, Department of Navy, Arlington, Virginia (1977).

2. Campbell, A. W., *Propellants, Explosives, Pyrotechnics* **9**, 183-187 (1984).

3. Tran, T. D., P. Lewis, J. Maeinschein, B. Druce, R. Lee and F. Roeske, *The 24th Aging, Compatibility and Stockpile Stewardship Conference Proceeding Volume*, Amarillo, Texas, April 30-May 2 (2002).

4 Tarver, C. M., *Propellants, Explosives and Pyrotechnics* **15**, 132 (1990).

5. P. Lewis, B. Cunningham, S. de Teresa and T. D. Tran. "Effects of thermal cycling on LX-17 and PBX 9502 density", *The 24th Aging, Compatibility and Stockpile Stewardship Conference Proceeding Volume*, Amarillo, Texas, April 30-May 2 (2002).

6. Dobratz, B. M., ed. LLNL Explosives Handbook, Chapter 8, UCRL-52997, Lawrence Livermore National Laboratory, Livermore, CA (1981).

7. Tarver, C. M., Hallquist, J. O., and Erickson, L. M., *Eighth Symposium (International) on Detonation*, Naval Surface Weapons Center NSWC 86-194, Albuquerque, NM, p. 951 (1985).

8. Urtiew, P. A., Erickson, L. M., Aldis, D. F., and Tarver, C. M., *Ninth Symposium (International) on Detonation*, Office of the Chief of Naval Research OCNR 113291-7, Portland, OR, p. 112 (1989).

9. Bahl, K., Bloom, G., Erickson, L., Lee, R., Tarver, C., Von Holle, W., and Weingart, R., *Eighth Symposium (International) on Detonation*, Naval Surface Weapons Center NSWC MP 86-194, Albuquerque, NM, p. 1045, (1985).

10. Urtiew, P. A., Cook, T. M., Maienschein, J. L., and Tarver, C. M., *Tenth International Detonation Symposium*, Office of Naval Research, ONR 33395-12, Boston, MA, p. 139, (1993).

11. Urtiew, P. A., Tarver, C. M., Maienschein, J. L., and Tao, W. C., *Combustion and Flame* **105**, 43 (1996).

12. Urtiew, P.A., Tarver, C. M., Forbes, J. W., and Garcia, F., *Shock Compression of Condensed Matter-1997*, S. C. Schmidt, D. P. Dandekar, J. W. Forbes, eds., AIP Conference Proceedings 429, Woodbury, NY, p. 727 (1998).

13. Tarver, C. M. and McGuire, E. M., paper presented at this Symposium.

14. Druce, R., Roeske, F., Fried, L., Souers, P. C., Tarver, C., Chow, C., Lee, R., McGuire, E., Overturf, G., Haskins, J., Schneberk, P., and Vitello, P., paper presented at this Symposium.

15. Price, D., J. *Energetic Materials* **1**, 55 (1983).